

See discussions, stats, and author profiles for this publication at: <https://www.researchgate.net/publication/231450395>

# Electronic energy levels in long polyenes: $S_2 \rightarrow S_0$ emission in all-trans-1,3,5,1,9,11,13-tetradecaheptaene

ARTICLE *in* JOURNAL OF THE AMERICAN CHEMICAL SOCIETY · JULY 1985

Impact Factor: 12.11 · DOI: 10.1021/ja00300a004

---

CITATIONS

63

---

READS

49

5 AUTHORS, INCLUDING:



Ronald L Christensen

Bowdoin College

50 PUBLICATIONS 1,742 CITATIONS

SEE PROFILE

## Electronic energy levels in long polyenes: S<sub>2</sub> → S<sub>0</sub> emission in all-trans-1,3,5,7,9,11,13-tetradecaheptaene

Richard Snyder, Eric Arvidson, Caroline Foote, Lynne Harrigan, and Ronald L. Christensen

*J. Am. Chem. Soc.*, **1985**, 107 (14), 4117-4122 • DOI: 10.1021/ja00300a004

Downloaded from <http://pubs.acs.org> on November 19, 2008

### More About This Article

---

The permalink <http://dx.doi.org/10.1021/ja00300a004> provides access to:

- Links to articles and content related to this article
- Copyright permission to reproduce figures and/or text from this article



ACS Publications  
High quality. High impact.

for nondilute quenchers. Using the Debye-Hückel potential  $\beta V_{DH} = z_A z_Q (r_c/r) e^{-\kappa r}$  ( $\kappa^2 = (2e^2 N_0 d \beta / 1000 \epsilon_0 \epsilon_r) I$ , with  $N_0$  Avagadro's number and  $d$  the solution density) in eq 4 leads to  $\bar{a}_{DH}/a = (r_c/a) \exp[-(r_c/a)(1 - \kappa a)]$  for like charged univalent ions with  $r_c/a \gg 1$ ; thus, the concentration effect is enhanced by increasing ionic strength. For oppositely charged univalent ions,  $\bar{a}_{DH}/a = (r_c/a) \exp(-\kappa r_c)$  and the concentration effect will be reduced relative to the zero ion strength result.<sup>14</sup> Both effects are present in the dilute case too, of course, and are due to the weakening of charge interactions by the Debye-Hückel screening. In room temperature water, for  $I = 0.01$  M  $\kappa = 3.3 \times 10^6$  cm<sup>-1</sup> and  $\kappa r_c = 0.233$ ; for a lower dielectric constant solvent (or more highly charged ions)  $\kappa r_c$  can be larger with a correspondingly greater effect.

In summary,  $1/\tau$  depends on  $\phi$  and  $\phi$  depends on  $\epsilon_r$  and  $I$ ; they must be properly accounted for when interpreting fluorescence quenching experiments.

The systematic calculation that we presented before<sup>7</sup> is restricted to the diffusion-controlled regime. We found that the result given

in eq 11 (for  $\nu \rightarrow \infty$ ) is the first correction to the dilute behavior; thus the approximate method given here yields the exact first correction. At higher concentration our previous calculation is also approximate. It yields the same general behavior as found here, in particular, both calculations predict  $k_f \sim (k_{DC})\bar{\phi}$  for large  $\bar{\phi}$ , but have different coefficients of proportionality.

We expect that the conclusions reached here for high  $\bar{\phi}$  values are qualitatively correct, but they should not be viewed as quantitative predictions. The possibility of a return to reaction control by increasing  $\bar{\phi}$  is especially intriguing. If this regime is accessible (oppositely charged ions in low  $\epsilon_r$  and  $I$  solutions) then the loss of chemical information that is a result of the diffusion-control limit can be bypassed. For example, electron-transfer reactions are difficult to study due to their rapidity ( $k_0$ , the actual transfer step is often large compared with  $k_D$ , the rate for diffusion). These reactions often are between inorganic ions of opposite charge and may become accessible by going to high quencher concentration.

**Acknowledgment.** I thank Professors P. J. Wagner and D. Nocera for their helpful comments. This work was supported by a grant from the National Science foundation (CHE 8318101).

(14) To obtain these simple connections between  $\bar{a}$  for Coulomb and Debye-Hückel potentials  $\kappa r_c$  must be small. See, for example, ref 1, p 167.

## Electronic Energy Levels in Long Polyenes: $S_2 \rightarrow S_0$ Emission in *all-trans*-1,3,5,7,9,11,13-Tetradecaheptaene

Richard Snyder, Eric Arvidson, Caroline Foote, Lynne Harrigan, and Ronald L. Christensen\*

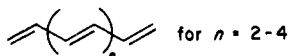
Contribution from the Department of Chemistry, Bowdoin College, Brunswick, Maine 04011.  
Received November 13, 1984

**Abstract:** Absorption, fluorescence, and fluorescence excitation spectra of *all-trans*-1,3,5,7,9,11,13-tetradecaheptaene have been obtained in room-temperature solutions and 77 K glasses. The heptaene, unlike shorter fluorescent polyenes, does not exhibit the characteristic gap between the origins of absorption ( $1^1A_g^- \rightarrow 1^1B_u^+$ ) and emission. Excitation spectra and solvent shift studies lead to the assignment of two distinct emissions,  $S_2 \rightarrow S_0$  ( $1^1B_u^+ \rightarrow 1^1A_g^-$ ) and  $S_1 \rightarrow S_0$  ( $2^1A_g^- \rightarrow 1^1A_g^-$ ), with the ratio of  $S_2$  to  $S_1$  emission increasing with the  $S_2$ - $S_1$  energy gap. Extrapolation of room-temperature solution data gives a gas-phase  $S_2$ - $S_1$  difference of 8400 cm<sup>-1</sup>. Tetradecaheptaene's "anomalous"  $S_2 \rightarrow S_0$  emission, the first observed for a linearly conjugated molecule, is compared to similar violations of Kasha's rule by azulene and other polyarenes. The spectroscopic and photochemical implications of these findings for other long polyenes also are discussed.

### I. Introduction

Recent research on linear polyenes ranges from theoretical investigations of the electronic states of model compounds to experiments which probe the initial photochemical events in vision and photosynthesis.<sup>1,2</sup> The optical spectroscopy of simple, unsubstituted polyene hydrocarbons has provided a fertile starting point for these other studies.<sup>3</sup> The model polyenes, both in 4.2 K mixed crystals and 77 K glasses, exhibit well-resolved (and thus informative) vibronic spectra. These spectra have established excited-state symmetries and have furnished some details of excited-state structures.

Previous work on unsubstituted *all-trans* polyenes



has shown that the lowest excited singlet state ( $2^1A_g^-$ ) diverges

from the second excited state ( $1^1B_u^+$ ) with increasing polyene length.<sup>4</sup> This behavior is not accounted for by current theories and raises the question of  $2^1A_g^-$ 's position in the long (i.e., "infinite") polyene limit. Does  $2^1A_g^-$  (like  $1^1B_u^+$ ) converge to a finite energy gap with respect to the electronic ground state ( $1^1A_g^-$ )? The experimental answer to this question poses an interesting challenge to theory and is closely related to such issues as the extent of bond alternation and the electronic properties of long polyene chains.<sup>5</sup> Extrapolation of our previous work to longer polyenes also could lead to the location and assignment of the electronic states of polyene natural products such as  $\beta$ -carotene ( $n = 9$ ). The position of  $\beta$ -carotene's low-energy electronic states is critical to an understanding of energy-transfer processes in photosynthesis.<sup>6</sup> Previous reports<sup>7</sup> of a low-lying  $2^1A_g^-$  state in

(4) D'Amico, K. L.; Manos, C.; Christensen, R. L. *J. Am. Chem. Soc.* **1980**, *102*, 1777.

(5) Ovchinnikov, A.; Ukrainiskii, I.; Krentsel, G. *Sov. Phys., Usp. (Engl. Transl.)* **1973**, *15*, 575. Yarkony, D. R.; Sibey, R. *Chem. Phys.* **1977**, *20*, 183.

(6) Govindjee, D. "Bioenergetics of Photosynthesis"; Academic Press: New York, 1975. Burnett, J. H. "Chemistry and Biochemistry of Plant Pigments"; Goodwin, T. W., Ed.; Academic Press: New York, 1976; Vol. 1, p 655.

(7) Thrash, R. J.; Fang, H.; Leroi, G. E. *J. Chem. Phys.* **1977**, *67*, 5930.

(1) Honig, B. *Annu. Rev. Phys. Chem.* **1978**, *29*, 31.  
(2) Birge, R. *Annu. Rev. Biophys. Bioeng.* **1981**, *10*, 315.  
(3) Hudson, B. S.; Kohler, B. E.; Schulten, K. In "Excited States"; Lim, E. C., Ed.; Academic Press: New York, 1982; Vol. 6, pp 1-95.



Figure 1. *all-trans*-1,3,5,7,9,11,13-Tetradecaheptaene.

$\beta$ -carotene are not consistent with the trends seen in shorter polyenes, and more work is needed to establish the electronic energy levels in long (and infinitely long) systems.

Simple extension of previous studies to longer systems ( $n > 4$ ) is handicapped by the precipitous reduction in emission yields with increasing polyene length.<sup>4</sup> For example, a previous attempt to obtain fluorescence and fluorescence excitation of tetradecaheptaene ( $n = 5$ , see Figure 1) did not succeed due to interfering emissions from hexaene impurities which were undetectable by absorption measurements. Further development of HPLC separation procedures and sample handling techniques now allow the collection of highly purified samples for low-temperature, spectroscopic studies. These procedures have enabled us to detect weak fluorescences in tetradecaheptaene and offer some hope of carrying out similar investigations of polyenes with  $n > 5$ . In addition to providing a better glimpse of the long polyene limit, our current work on the heptaene also gives some insight into problems in detecting the low-lying  $2^1A_g$  state in shorter polyenes in the gas phase.

## II. Experimental Section

**Synthesis and Purification of *all-trans*-1,3,5,7,9,11,13-Tetradecaheptaene.** The heptaene was prepared by the acid-catalyzed dehydration of *all-trans*-1,4,6,8,10,12-tetradecaheptaen-3-ol. The hexaenol was obtained by the Grignard addition of vinylmagnesium bromide to 2,4,6,8,10-dodecapentaenal.

Dodecapentaenal was synthesized from crotonaldehyde (Aldrich) as described previously.<sup>4,8</sup> Dodecapentaenal (1.2 g) was then dissolved in 150 mL of THF. This solution was slowly stirred into 20 mL of a 1 M solution of vinylmagnesium bromide in THF (Alpha) which had been placed in an ice bath. The reaction was monitored by UV absorption and came to completion in  $\sim 15$  min. The excess Grignard was decomposed by repeated washings with a saturated aqueous solution of ammonium chloride followed by washings with aqueous sodium bicarbonate. The hexaenol then was dried over anhydrous sodium sulfate and stored at  $-10^\circ\text{C}$ .

The alcohol solution was subjected to rotary evaporation and reconstituted in 500 mL of chloroform. Chloroform (1 mL) saturated with HCl(g) was added dropwise with stirring to the room-temperature reaction mixture until the 390 nm absorbance peak of the expected heptaene product reached its maximum intensity. At this point ( $\sim 20$  min) the reaction was quenched by repeated washings with water and dilute aqueous sodium bicarbonate. The chloroform layer was then dried with anhydrous sodium sulfate.

The dehydration products were redissolved in 10 mL of hexane/ether (3/1, v/v) and loaded on to a chromatography column (2.5-cm diameter) containing 10 cm of Woelm neutral alumina (activity grade II). Elution with hexane/ether (3/1) removed the hydrocarbon fractions with the collection being terminated at the point where the 390-nm absorbance became negligible. The ratio of 390-nm absorbance to 370-nm absorbance in the collected fractions was  $\sim 1/10$ , indicating the dominance of shorter polyene hydrocarbons. This mixture was reconstituted in hexane and loaded onto a second chromatography containing 15 cm of Woelm neutral alumina (activity grade II). Elution with hexane separated the heptaene from shorter polyene impurities. The absorption spectra of the heptaene fractions were comparable to those given by Mebane<sup>9</sup> and indicated an overall yield (starting from dodecapentaenal) of about 0.5%.

The final stage of purification was carried out by HPLC with a reversed phase column (Altex Ultrasphere-ODS, 4.6 mm  $\times$  25 cm) and a mobile phase of methanol/water (4/1, v/v). Injections (20  $\mu\text{L}$ ) of the concentrated heptaene and collection of single elution peaks provided samples with absorptions sufficient for spectroscopic studies. Reinjection of the major heptaene peak (occurring at  $\sim 30$  min and assigned to the *all-trans* configuration) indicates the facile formation of degradation products (including isomers) whose presence cannot be detected by simple inspection of the UV absorption spectrum. Our purest samples were obtained by collecting samples with the HPLC detector (365 nm mercury emission line) turned off during elution and collection of the heptaene peak. The methanol/water solutions were extracted with hexane for

room-temperature spectroscopy. For low-temperature spectra, the hexane solutions were evaporated in a stream of nitrogen and immediately redissolved in EPA (ether/isopentane/ethanol, 5/2/2, MCB). The entire procedure by which an HPLC peak was collected and converted to a low-temperature sample was carried out as rapidly as possible under subdued lights in order to minimize fluorescence from heptaene degradation products. Sample purities were monitored by reinjection of samples before and after spectroscopic measurements.

**Synthesis and Purification of *all-trans*-1,3,5,7,9,11-Dodecahexaene.** The hexaene was prepared by the acid-catalyzed dehydration of *all-trans*-2,4,6,8,10-dodecapentaen-1-ol which was obtained by reduction of 2,4,6,8,10-dodecapentaenal.

Dodecapentaenal (150 mg) was dissolved in 500 mL of methanol. A twofold molar excess of NaBH<sub>4</sub> was slowly added and the solution stirred for 15 min. Dodecapentaenol (obtained in  $\sim 100\%$  yield) was recrystallized from ethanol to give pale yellow crystals with a melting point of 203–205  $^\circ\text{C}$ , in good agreement with Fischer et al.<sup>10</sup>

Dodecapentaenol (100 mg) was dissolved in 500 mL of chloroform and subjected to the HCl dehydration procedures described above. The dehydration was run until the hexaene absorption at 375 nm reached a maximum. The reaction was then quenched and chromatographed on alumina (first with hexane/ether then with pure hexane) as described for the heptaene. *all-trans*-Dodecahexaene was then separated and collected with C<sub>18</sub> reversed phase HPLC and methanol/water (4/1) as described above. Starting from dodecapentaenal, the overall yield of hexaene was  $\sim 5\%$ . UV absorption spectra of the final hexaene fractions were in good agreement with those given by Sondheimer et al.<sup>11</sup>

**Spectral Measurements.** Absorption spectra were obtained on a Perkin-Elmer Lambda 3 UV-visible spectrophotometer which had been modified for 77 K measurements. The spectral resolution of the absorption spectra was 2 nm as limited by the fixed slits of the Lambda 3. Absorbances from the Lambda 3 were stored on a microcomputer (Digital Equipment Corporation MINC-11) for subsequent manipulation and display.

Fluorescence and fluorescence excitation spectra were obtained on a home-built fluorimeter and stored on the MINC-11 computer as described previously.<sup>8</sup> Spectral band widths, filtering conditions, etc., are indicated on the spectra. Certain of the heptaene fluorescence spectra were excited with the 405.4-nm line from a 100-W mercury lamp. For these spectra the excitation monochromator was replaced by a filter combination consisting of 10 cm of water, a Corning 7-54 glass filter, and a Dittic Optics 410 nm, 10 nm band-pass interference filter.

Fluorescence and fluorescence excitation spectra were corrected for the wavelength-dependent efficiencies of the excitation and emission monochromators, photomultiplier, and collection optics. The *emission correction* curve was obtained by recording the output of a Tungsten lamp whose spectrum had been calibrated (in quanta/nm) against NBS standards. The correction procedures were evaluated by comparing spectra detected with two rather different photomultipliers (a "blue" sensitive tube, EMI 6256S, and a "red" sensitive tube, Hamamatsu 928). The corrected spectra obtained with these tubes were essentially identical for 300 nm  $< \lambda < 600$  nm. The *excitation correction* curve was acquired by recording the excitation spectrum off the front face of a triangular cuvette containing an "optically thick" solution of Rhodamine B (5 g/L of ethylene glycol). Monitoring the Rhodamine B emission at 600 nm provided an excitation correction curve for 300 nm  $< \lambda < 600$  nm. The corrected excitation spectra of several dilute standard solutions (anthracene, perylene, fluorescein, and Rhodamine B) were in good agreement with absorption spectra obtained on a Beckman 24 UV-visible spectrophotometer.

Prior to scaling and replotting, the emission spectra were smoothed to reduce the noise inherent in these weakly emitting systems. The smoothing routine employed, an 11 point Savitsky-Golay fit to a cubic,<sup>12,13</sup> only minimally distorted the vibronic features described in this paper.

## III. Results

The 77 K absorption and emission spectra of *all-trans*-1,3,5,7,9,11,13-tetradecaheptaene will be compared with the spectra of *all-trans*-1,3,5,7,9,11-dodecahexaene, the next shortest member of this hydrocarbon series. This comparison will be useful in linking the present study to our previous work on shorter systems. Low-temperature spectra of both the hexaene and

(10) Fischer, F. G.; Hultsch, K.; Flaig, W. *Berichte* 1937, 70, 370.

(11) Sondheimer, F.; Ben-Efraim, D.; Wolovsky, R. *J. Am. Chem. Soc.* 1961, 83, 1675.

(12) Savitzky, A.; Golay, M. J. E. *Anal. Chem.* 1964, 36, 1627.

(13) Steiner, J.; Termonia, Y.; Deltour, J. *Anal. Chem.* 1972, 44, 1906.

(8) Palmer, B.; Jumper, B.; Hagan, W.; Baum, J. C.; Christensen, R. L. *J. Am. Chem. Soc.* 1982, 104, 6907.

(9) Mebane, A. D. *J. Am. Chem. Soc.* 1952, 74, 5227.

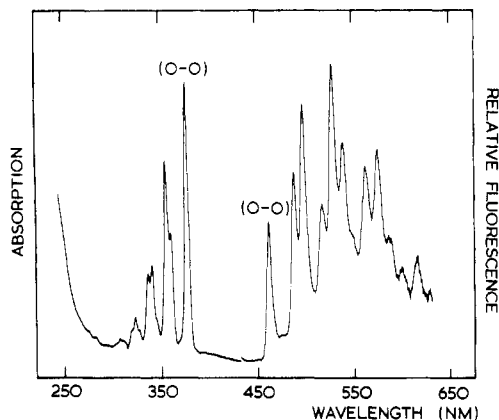


**Figure 2.** Absorption and fluorescence spectra of *all-trans*-1,3,5,7,9,11-dodecahexaene in 77 K EPA. Absorption spectra obtained with a 2 nm band-pass. Fluorescence excited at  $380 \pm 5$  nm and detected with 1 nm resolution through a Schott KV-418 filter.

heptaene have awaited the purification levels afforded by HPLC techniques. Previous work has shown that these longer polyenes tend to precipitate in low-temperature glasses, causing their spectra to be dominated by shorter, more fluorescent polyene impurities.<sup>4</sup> Our separation procedures have made significant improvements on these earlier results.

The 77 K absorption and fluorescence spectra of the dodecahexaene are presented in Figure 2. The corrected fluorescence excitation spectrum is in good agreement with the absorption spectrum, and the fluorescence spectrum is independent of the excitation wavelength. These observations confirm that we are dealing with a single-component sample. The hexaene spectra are very similar to 77 K spectra previously obtained for 1,3,5,7,9-decapentaene and 1,3,5,7-octatetraene<sup>4</sup> and can be described by a scheme involving the ground electronic state ( $1^1A_g$ ) and two closely lying excited states ( $2^1A_g$  and  $1^1B_u^+$ ).<sup>3</sup> Thus, the strong absorption ((0-0) at 376 nm) corresponding to  $1^1A_g \rightarrow 1^1B_u^+$  is followed by relaxation to a lower lying  $2^1A_g$  state. Fluorescence due to the forbidden transition ( $2^1A_g \rightarrow 1^1A_g$ ) occurs with a (0-0) at 461 nm. The  $4900\text{-cm}^{-1}$  gap between the absorption and emission origins in Figure 2 thus corresponds to the energy difference between the two lowest excited states. This energy level scheme is well supported by a variety of one- and two-photon optical measurements.<sup>2,3</sup>

The 77 K absorption and fluorescence spectra of tetradecaheptaene are given in Figure 3. Comparison of the corrected excitation and absorption spectra and the observation that the fluorescence spectrum is not strictly independent of excitation wavelength indicate that, even in these highly purified samples, there are emissions from shorter polyenes (those with fewer than seven conjugated bonds) absorbing at  $\lambda \leq 390$  nm. Nevertheless, the heptaene emission can be isolated by pumping the absorption (0-0) at 402 nm. This results in the relatively intense, well-resolved fluorescence given in Figure 3. Excitation into higher energy vibronic bands (e.g., the strong vibronic feature at 383 nm) gives emissions with decreased resolution and increased intensity at shorter wavelengths. A series of fluorescence spectra taken over a broad range of excitation wavelengths was used to establish the emission (0-0) at 408 nm. Similarly, a survey of excitation spectra as a function of emission wavelength gave a series of spectra which reproduce all the vibronic features of the heptaene absorption, including the electronic origin (402 nm).

The interferences from shorter polyene impurities arise as much from their relatively large fluorescence efficiencies as from their concentrations (no more than a few percent relative to the heptaene). As we have noted previously,<sup>4</sup> polyene low-temperature fluorescence yields decrease from 0.6 in octatetraene to about 0.01 in dodecahexaene. Lacking more quantitative information, we estimate the heptaene emission yield to be 0.001. These trends clearly underscore the problems in obtaining heptaene emission and excitation spectra which are not contaminated by spectra of shorter, more fluorescent impurities. In spite of these problems,

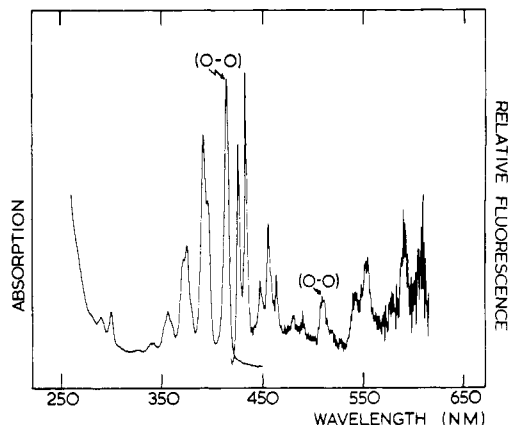


**Figure 3.** Absorption and fluorescence spectra of *all-trans*-1,3,5,7,9,11,13-tetradecaheptaene in 77 K EPA. Absorption obtained with a 2 nm band-pass. Fluorescence excited at 405.4 nm and detected with 1 nm resolution through a Schott KV-418 filter.

a systematic investigation of fluorescence intensity as a function of both exciting and emitting wavelengths provides the necessary link between heptaene absorption and the fluorescence spectrum presented in Figure 3.

The 77 K spectra of tetradecaheptaene (Figure 3) provide some interesting contrasts to the spectra of dodecahexaene (Figure 2). The most obvious difference is the apparent absence of an energy gap between the onset of absorption and the onset of emission. The 6-nm ( $370\text{ cm}^{-1}$ ) difference between the absorption and emission peaks is comparable to the small Stokes shifts observed for many other systems<sup>14</sup> and can be explained by our inability to resolve phonon and low-frequency vibronic structure in these spectra. We thus must conclude that in contrast to the hexaene, emission occurs from the  $1^1B_u^+$  state reached by direct absorption.

The heptaene fluorescence spectrum also exhibits some weak, but reproducible vibronic features at  $\lambda \geq 511$  nm. Excitation spectra monitored on these bands correspond closely to the absorption spectrum (e.g., the feature at 402 nm is reproduced), although there still are interferences from shorter polyene (e.g., hexaene) emissions. The location of the weak heptaene emission, the vibronic patterns observed, and the correspondence between the excitation and absorption spectra all suggest that this second emission is due to the  $2^1A_g \rightarrow 1^1A_g$  transition observed for shorter polyenes. The heptaene spectra thus require emission from both  $S_2$  ( $1^1B_u^+$ ) and  $S_1$  ( $2^1A_g$ ) with  $S_2 \rightarrow S_0$  emission dominating.

Solvent effects on room-temperature absorption and emission spectra confirm these assignments of tetradecaheptaene's lowest energy electronic transitions. The transition energies can be fit to the following equation<sup>3,4,15,16,17</sup>

$$\bar{\nu}(\text{solvent}) = \bar{\nu}(\text{gas}) - k(n^2 - 1)/(n^2 + 2)$$

where  $k$  is a coefficient related to the strength of the transition,  $n$  is the index of refraction, and  $\bar{\nu}(\text{gas})$  is the transition origin (0-0) under gas-phase conditions. Least-squares fits to room-temperature absorption and fluorescence origins are presented in Table I. Data for the heptaene are compared with previous solvent shift data for the three shorter members of this series. The studies show that heptaene's 402 nm absorption band and 408 nm emission band have parallel solvent shifts with  $k$ 's comparable to those previously obtained for the allowed ( $1^1A_g \rightarrow 1^1B_u^+$ ) transition in shorter polyenes.<sup>4</sup> The 511-nm band, on the other hand, has a much smaller shift coefficient, indicative of a forbidden transition ( $2^1A_g \rightarrow 1^1A_g$ ).<sup>3,4</sup> Other weak spectral features with  $\lambda < 511$  nm (e.g., the bands from 480 to 490 nm) also might be considered as candidates for the  $S_1 \rightarrow S_0$  (0-0). These emissions, however, have

(14) Berlman, I. B. "Handbook of Fluorescence Spectra of Aromatic Molecules"; Academic Press: New York, 1965.

(15) Basu, S. *Adv. Quantum Chem.* **1964**, *1*, 145.

(16) Andrews, J.; Hudson, B. *J. Chem. Phys.* **1978**, *68*, 4587.

(17) Gavin, R. M., Jr.; Weisman, C.; McVey, J. K.; Rice, S. A. *J. Chem. Phys.* **1978**, *68*, 522.

**Table I.** Solvent Effects on Polyene Transition Energies:  $\bar{\nu}(\text{solvent}) = \bar{\nu}(\text{gas}) - k(n^2 - 1)/(n^2 + 2)$ 

	absorption ( $S_0 \rightarrow S_2$ )		emission ( $S_2 \rightarrow S_0$ )		emission ( $S_1 \rightarrow S_0$ )		extrapolated energy gap <sup>f</sup> $\Delta\bar{\nu}(0-0)$ , $\text{cm}^{-1}$
	$\bar{\nu}(\text{gas})$ , $\text{cm}^{-1}$	$k$ , $\text{cm}^{-1}$	$\bar{\nu}(\text{gas})$ , $\text{cm}^{-1}$	$k$ , $\text{cm}^{-1}$	$\bar{\nu}(\text{gas})$ , $\text{cm}^{-1}$	$k$ , $\text{cm}^{-1}$	
tetradecaheptaene <sup>a</sup>	28 530 <sup>d</sup> $\pm$ 150 <sup>e</sup>	12 110 $\pm$ 600	27 890 $\pm$ 200	10 300 $\pm$ 500	19 840 $\pm$ 140	1690 $\pm$ 560	8690 $\pm$ 290
dodecahexaene <sup>b</sup>	29 450 $\pm$ 300	9 260 $\pm$ 1140			22 030 $\pm$ 90	1570 $\pm$ 360	7420 $\pm$ 320
decapentaene <sup>b</sup>	32 080 $\pm$ 330	9 640 $\pm$ 1290			25 020 $\pm$ 160	2160 $\pm$ 340	7060 $\pm$ 370
octatetraene <sup>c</sup>	35 350 $\pm$ 250	10 910 $\pm$ 1000			28 970 $\pm$ 100	1690 $\pm$ 400	6380 $\pm$ 270

<sup>a</sup>Solvents used: *n*-pentane, *n*-hexane, *n*-hexadecane, benzene. <sup>b</sup>Data from D'Amico et al., ref 4. <sup>c</sup>Data from Gavin et al., ref 17. <sup>d</sup> $\bar{\nu}$ 's refer to transition energies of (0-0)'s. <sup>e</sup>Errors are given as  $\pm 1\sigma$ . <sup>f</sup>Energy is the difference between absorption ( $S_0 \rightarrow S_2$ ) and emission ( $S_1 \rightarrow S_0$ ) extrapolated origins.

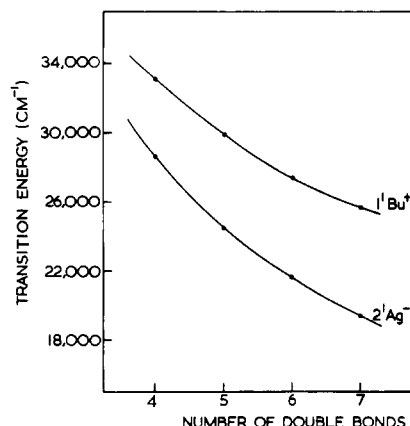


**Figure 4.** Comparison of  $1^1A_g^- \rightarrow 2^1A_g^-$  and  $1^1A_g^- \rightarrow 1^1B_u^+$  transition energies ((0-0)'s) of unsubstituted polyene hydrocarbons in 25 °C *n*-hexane (references: octatetraene (4 and 17), decapentaene (4 and 9), dodecahexaene (4 and 11), tetradecaheptaene (9 and this work)).

solvent shifts of allowed transitions. This observation plus the now familiar vibronic patterns of the long-wavelength ( $\lambda \geq 511$  nm) emissions (e.g., compared with the hexaene fluorescence seen in Figure 2) lead to the assignment of the 511-nm peak as the  $S_1 \rightarrow S_0$  electronic origin.

The heptaene solvent shift data, in addition to providing crucial guidance for state assignments, also allow us to extend our previous investigation of the dependence of transition energies on polyene length. Data for a common solvent (*n*-hexane) are summarized in Figure 4. The gas-phase energy difference between  $1^1B_u^+$  and  $2^1A_g^-$  as a function of polyene length is given in Figure 5. Both plots show a systematic divergence between the two excited states with increasing conjugation.

#### IV. Discussion of Results

The spectra presented in the previous section can be described by the three-level energy scheme ( $1^1B_u^+ > 2^1A_g^- > 1^1A_g^-$ ) developed for the electronic states of shorter all-trans polyene hydrocarbons ( $n \geq 2$ ). This model is based on a large body of spectroscopic data and has been the subject of recent review.<sup>2,3</sup> Several of these molecules (e.g., octatetraene,<sup>17-20</sup> dimethyloctatetraene,<sup>21</sup> 2,10-dimethylundecapentaene,<sup>22,23</sup> 2,12-dimethyltridecahexaene,<sup>24,25</sup> etc.) have been investigated in particular detail. One- and two-photon high-resolution optical spectra, lifetime and quantum yield measurements, studies of solvent effects on spectra, etc., all require that the symmetry-allowed  $S_0 \rightarrow S_2$  absorption ( $1^1A_g^- \rightarrow 1^1B_u^+$ ) be followed by a symmetry-forbidden  $S_1 \rightarrow S_0$  emission ( $2^1A_g^- \rightarrow$

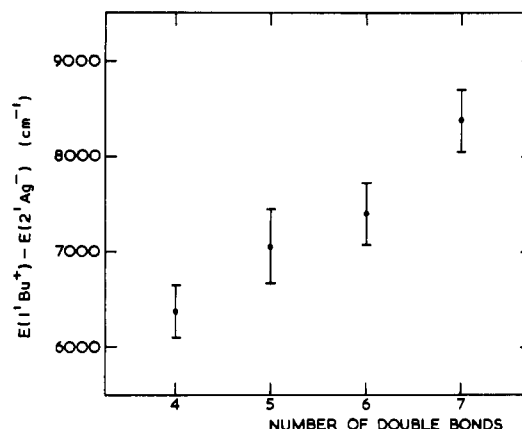


**Figure 5.** Extrapolated, gas-phase energy differences between  $1^1B_u^+$  and  $2^1A_g^-$  states in unsubstituted tetraene,<sup>17</sup> pentaene,<sup>4</sup> hexaene,<sup>4</sup> and heptaene (this work). Error bars are  $\pm 1\sigma$  and are calculated from errors in  $\bar{\nu}(\text{gas}, S_0 \rightarrow S_2)$  and  $\bar{\nu}(\text{gas}, S_1 \rightarrow S_0)$  given in Table I.

$1^1A_g^-$ ). The ordering of the three lowest singlet states is thus well established for molecules comparable to *all-trans*-dodecahexaene and *all-trans*-tetradecaheptaene.<sup>3</sup>

The primary conclusions of this paper are based on the unexpected differences between the fluorescence properties of the hexaene and heptaene (Figures 2 and 3). The hexaene exhibits the typically large "Stokes-shift" between the strongly allowed absorption and the origin of the fluorescence. This shift is one of the primary signatures of polyene spectroscopy, having been observed for all fluorescent all-trans polyene hydrocarbons ( $n \geq 2$ ). The forbidden,  $S_0 \rightarrow S_1$  absorption has been detected for several polyenes, and the coincidence between the origin of the weak,  $1^1A_g^- \rightarrow 2^1A_g^-$  absorption and the origin of fluorescence provides additional verification of the state assignments. However, the simple observation of a gap between fluorescence and the strong  $1^1A_g^- \rightarrow 1^1B_u^+$  absorption provides the experimentally most convenient, most direct evidence that  $1^1B_u^+ > 2^1A_g^- > 1^1A_g^-$  for the hexaene and a large number of other molecules.

Tetradecaheptaene is the first all-trans polyene hydrocarbon in condensed phase which does not exhibit a Stokes shift between the origin of the  $1^1A_g^- \rightarrow 1^1B_u^+$  transition and the origin of fluorescence. This requires that the "resonance" fluorescence ((0-0) at 408 nm) be assigned as  $S_2 \rightarrow S_0$  ( $1^1B_u^+ \rightarrow 1^1A_g^-$ ).  $1^1B_u^+$  cannot be the lowest excited singlet because of trends observed in the shorter polyenes and the expectation that the energy levels of polyenes should vary smoothly with increasing conjugation.<sup>3,5,26</sup> Thus, for  $n = 2-4$ , the  $1^1B_u^+ - 2^1A_g^-$  gap shows an increase with polyene length which extrapolates to  $>6000 \text{ cm}^{-1}$  in the heptaene. It is important to emphasize that the solvent dependence of the 408-nm emission ( $k \sim 10\,000 \text{ cm}^{-1}$ ; Table I) eliminates the possibility that the emission is due to  $2^1A_g^- \rightarrow 1^1A_g^-$  transitions of shorter polyene impurities. Tetradecaheptaene is thus the first linearly conjugated system that has been observed to violate Kasha's rule.

This conclusion is reinforced by our observation of a second, weak emission at  $\lambda \geq 511$  nm. These vibronic features, the lowest energy emissions yet observed for an all-trans<sup>27</sup> polyene

(18) Granville, M. F.; Holtom, G. R.; Kohler, B. E.; Christensen, R. L.; D'Amico, K. L. *J. Chem. Phys.* **1979**, *70*, 593.

(19) Granville, M. F.; Holtom, G. R.; Kohler, B. E. *J. Chem. Phys.* **1981**, *74*, 4.

(20) Heimbrook, L. A.; Kohler, B. E.; Levy, I. J. *J. Chem. Phys.* **1984**, *81*, 1592.

(21) Andrews, J.; Hudson, B. *Chem. Phys. Lett.* **1978**, *57*, 600.

(22) Christensen, R. L.; Kohler, B. E. *Photochem. Photobiol.* **1973**, *18*, 293.

(23) Christensen, R. L.; Kohler, B. E. *J. Chem. Phys.* **1975**, *63*, 1837.

(24) Christensen, R. L.; Kohler, B. E. *J. Phys. Chem.* **1976**, *80*, 2197.

(25) Auerbach, R. A.; Christensen, R. L.; Granville, M. F.; Kohler, B. E. *J. Chem. Phys.* **1981**, *74*, 4.

(26) Tavan, P.; Schulten, K. *J. Chem. Phys.* **1979**, *70*, 5407.

hydrocarbon, are assigned to  $2^1A_g^- \rightarrow 1^1A_g^-$  ( $S_1 \rightarrow S_0$ ). The vibronic structure observed is comparable to that seen in the emission spectra of shorter polyenes. Excitation spectra of these bands reproduce the excitation spectra obtained on the bands originating at 411 nm. In addition, the solvent shifts of the long-wavelength emission ( $k \sim 1700 \text{ cm}^{-1}$ ) are typical of those observed for electronically forbidden polyene transitions.<sup>3,4</sup> The relatively low fluorescent quantum yield continues the trend observed for shorter members of the hydrocarbon series ( $n = 2-4$ ) and presumably reflects the increased efficiency of  $S_1 \rightarrow S_0$  internal conversion due to the smaller  $2^1A_g^- - 1^1A_g^-$  energy difference. These trends suggest that  $2^1A_g^- \rightarrow 1^1A_g^-$  emission for polyenes with  $n > 5$  will be even more difficult to detect. The dual emission of the heptaene thus may serve as the bridge between the shorter polyenes ( $S_1 \rightarrow S_0$  emission only) and longer polyenes ( $S_2 \rightarrow S_0$  emission only). It should be stressed, however, that the detection of  $2^1A_g^- \rightarrow 1^1A_g^-$  emission would not be necessary for the verification of the  $1^1B_u^+ > 2^1A_g^- > 1^1A_g^-$  energy scheme and  $S_2 \rightarrow S_0$  emission in longer polyene systems.

Improved purification and sample-handling techniques might lead to better excitation spectra and further proof of the heptaene state assignments. However, tetradecaheptaene's low solubility, low  $S_0 \rightarrow S_1$  extinctions ( $< 100 \text{ L mol}^{-1} \text{ cm}^{-1}$ ), and low fluorescence yields would make direct excitation of  $S_1 \rightarrow S_0$  emission a rather difficult task. Such measurements might be feasible under the high-resolution conditions provided by low-temperature (4.2 K) polyene/*n*-alkane mixed crystals.<sup>18,23,24</sup> High-resolution excitation and emission spectra could demonstrate the coincidence between  $S_0 \leftrightarrow S_1$  and  $S_0 \leftrightarrow S_2$  absorption and emission electronic origins. High-resolution fluorescence spectra also could show that the 408- and 511-nm emissions terminate in common vibronic states.

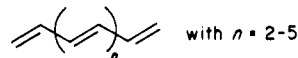
$S_2 \rightarrow S_0$  emission from large molecules in condensed phases was first observed for azulene by Beer and Longuet-Higgins.<sup>28</sup> Similar violations of Kasha's rule were subsequently observed for derivatives of azulene,<sup>29,30</sup> metalloporphyrins,<sup>31,32</sup> and several polyacenes.<sup>33,34</sup> All of these systems are characterized by relatively large energy differences between their first and second excited singlets (e.g.,  $14000 \text{ cm}^{-1}$  in azulene,<sup>30</sup>  $6900 \text{ cm}^{-1}$  in Zn tetraphenylporphyrin,<sup>31</sup> and  $7000 \text{ cm}^{-1}$  in acenanthrylene<sup>34</sup>).  $S_2 \rightarrow S_0$  emission is then explained by the relatively small Franck-Condon factors associated with  $S_2 \rightarrow S_1$  internal conversion.  $S_2$  emission also is favored for molecules such as those cited above where  $S_2 \rightarrow S_0$  is an allowed (short lifetime) transition.

Linear polyenes are, in hindsight, rather well-suited for violating Kasha's rule. The widening of the  $S_2-S_1$  energy gap ( $\Delta E$ ) with increasing conjugation should be accompanied by a decrease in the  $S_2 \rightarrow S_1$  internal conversion rate ( $k_{ic}$ ). In addition, the symmetry-allowed  $S_0 \leftrightarrow S_2$  ( $1^1A_g^- \leftrightarrow 1^1B_u^+$ ) transition provides for fast  $S_2$  radiative decay ( $k_r \sim 10^9 \text{ s}^{-1}$ ). Polyenes thus should reach a length where fluorescence from  $S_2$  (quantum yield =  $k_r/(k_r + k_{ic})$  in the absence of intersystem crossing) reaches a detectable level. The change from  $S_1 \rightarrow S_0$  to  $S_2 \rightarrow S_0$  fluorescence appears to have been reached in going from dodecaheptaene to tetradecaheptaene. The difference between the emission of the hexaene ( $\Delta E = 4900 \text{ cm}^{-1}$  in 77 K EPA) and the emission of the heptaene ( $\Delta E = 5320 \text{ cm}^{-1}$  in 77 K EPA) indicates that  $k_{ic}$  is rather sensitive to the  $S_2-S_1$  energy difference. While the heptaene retains some vestiges of  $S_1 \rightarrow S_0$  fluorescence,  $S_1$  emission may be effectively

eliminated for the larger  $S_2-S_1$  gaps associated with longer systems ( $n > 5$ ).

The theoretical basis for  $S_2 \rightarrow S_0$  fluorescences in azulene and other cyclic aromatic hydrocarbons has been given by Englman and Jortner.<sup>35</sup> Certain aspects of this theory, e.g., that  $k_{ic}$  should vary exponentially with  $\Delta E$ , have been verified by experiment.<sup>29,32</sup> The linear polyenes obviously would provide some interesting tests of models for radiationless decay in conjugated systems. The  $S_2-S_1$  energy gap in polyenes could be carefully tuned by changing the refractive index of the solvent (see Table I), adding substituents, or changing the length of conjugation. For example, we have seen a fourfold decrease in the ratio of  $S_1 \rightarrow S_0$  to  $S_2 \rightarrow S_0$  emission in changing from heptaene in benzene ( $\Delta E = 5650 \text{ cm}^{-1}$ ) to an *n*-pentane ( $\Delta E = 6420 \text{ cm}^{-1}$ ) solution. The striking differences between the low-temperature fluorescences of dodecaheptaene and tetradecaheptaene also have been noted. These observations do not provide a direct measure of the rate of excited-state internal conversion ( $k_{ic}$ ) in these system, but they do indicate  $k_{ic}$ 's rather steep dependence on  $\Delta E$  in the  $4500-6500 \text{ cm}^{-1}$  region. A more quantitative discussion of radiationless decay in the heptaene awaits lifetime and quantum-yield data. Our preliminary observations, however, indicate some interesting parallels with azulene and other cyclic systems.

The dual fluorescences from room-temperature solutions of tetradecaheptaene allow the extrapolation of electronic energies to gas-phase conditions (Table I) and extend our previous study on the dependence of  $1^1B_u^+$  and  $2^1A_g^-$  energies on polyene length.<sup>4</sup> Figure 4 compares  $1^1A_g^- \rightarrow 1^1B_u^+$  and  $2^1A_g^- \rightarrow 1^1A_g^-$  transition energies in room-temperature *n*-hexane for polyenes



The gas-phase differences between  $1^1B_u^+$  and  $2^1A_g^-$  (i.e.,  $\Delta E = S_2 - S_1$ ) are given in Figure 5. Both plots indicate a divergence of  $2^1A_g^-$  and  $1^1B_u^+$  with increasing conjugation. The  $1^1B_u^+$  state approaches a finite energy limit for long polyenes (Figure 4). The data in hand, however, give no indication of a similar, nonzero, long polyene limit for  $2^1A_g^-$ . This behavior is not accounted for by current theories of polyene electronic structure,<sup>5,36</sup> and clearly it has some interesting implications for the photophysical and photochemical properties of long (e.g.,  $\beta$ -carotene) and infinitely long (e.g., polyacetylene) polyene systems.

Before speculating on these longer polyenes, we first shall consider how the observation of  $S_2 \rightarrow S_1$  fluorescence and the trends seen in Figures 4 and 5 relate to radiative decay in short polyenes. One outstanding problem is the absence of  $2^1A_g^- \rightarrow 1^1A_g^-$  emission in gas-phase octatetraene.<sup>17,20</sup> This transition has high yield ( $\phi_f \sim 0.8$ ) and is well characterized in low-temperature glasses and mixed crystals, but vapor-phase samples only give resonant fluorescence ( $1^1B_u^+ \rightarrow 1^1A_g^-$ ) upon absorption into  $1^1B_u^+$ . This difference has led to the suggestion<sup>17,37</sup> that the low-energy, Stokes-shifted fluorescences in octatetraene and other polyenes in condensed phases are experimental artifacts which do not apply to isolated, gas-phase molecules. One possibility is that the low-energy emissions arise from other conformers of the parent polyene. This explanation has some appeal in foregoing the theoretical difficulties both in accounting for  $1^1B_u^+ > 2^1A_g^-$  and in explaining the long polyene trends noted in Figures 4 and 5.

Our experiments on tetraheptaene explain  $S_2 \rightarrow S_0$  emission in vapor-phase octatetraene. Analysis of room-temperature solvent shifts indicates a  $6400 \text{ cm}^{-1}$   $1^1B_u^+ - 2^1A_g^-$  energy gap in gaseous octatetraene. This energy difference should be compared with the  $6300\text{-cm}^{-1}$   $\Delta E$  for the heptaene in *n*-hexane. We thus expect similar  $S_2 \rightarrow S_1$  internal conversion rates and the gas-phase emission of octatetraene to be dominated by  $S_2 \rightarrow S_0$  emission. On the other hand, octatetraene in *n*-hexane (or similar hydrocarbon solvents) has a  $\Delta E = 4200 \text{ cm}^{-1}$  (cf.,  $\Delta E = 4900 \text{ cm}^{-1}$  for

(27) Bridged, "hairpin" polyenes fluoresce at wavelengths longer than those of the all-trans polyenes discussed here. (Frölich, W.; Dewey, H.; Deger, H.; Dick, B.; Klingensmith, K.; Pittman, W.; Vogel, E.; Hohlneicher, G.; Michl, J. *J. Am. Chem. Soc.* **1983**, *105*, 6211.)

(28) Beer, M.; Longuet-Higgins, H. C. *J. Chem. Phys.* **1955**, *23*, 1390.

(29) Maurata, S.; Iwanaga, C.; Toda, T.; Kokubun, H. *Chem. Phys. Lett.* **1972**, *13*, 101.

(30) Eber, G.; Schneider, S.; Dörr, F. *Chem. Phys. Lett.* **1977**, *52*, 59.

(31) Bajema, K.; Gouterman, M.; Rose, C. B. *J. Mol. Spectrosc.* **1971**, *39*, 421.

(32) Kurabayashi, Y.; Kikuchi, K.; Kokubun, H.; Kaizu, Y.; Kobayashi, H. *J. Phys. Chem.* **1984**, *88*, 1308.

(33) Leupin, W.; Berens, S.; Magde, D.; Wirz, J. *J. Phys. Chem.* **1984**, *88*, 1376.

(34) Plummer, B.; Al-Saigh, Z.; Arfan, M. *Chem. Phys. Lett.* **1984**, *104*, 389.

(35) Englman, R.; Jortner, J. *Mol. Phys.* **1970**, *18*, 145.

(36) Tavan, P.; Schulten, K. *J. Chem. Phys.* **1979**, *70*, 5407.

(37) McDiarmid, R. *J. Chem. Phys.* **1983**, *79*, 9.

dodecahexaene in 77 K EPA) and thus should exhibit normal,  $S_1 \rightarrow S_0$  fluorescence. The comparison with the heptaene does not explain the complete absence of  $2^1A_g^-$  emission in the gaseous octatetraene. This may be due to even smaller internal conversion rates in isolated, gas-phase molecules and/or a reduced radiative decay from  $S_1$  due to the absence of solvent perturbations on the symmetry-forbidden  $2^1A_g^- \rightarrow 1^1A_g^-$  transition. With the addition of these details, the difference in emission between gaseous and condensed-phase octatetraene can be accounted for by the large change in the rate of  $S_2 \xrightarrow{\text{w}} S_1$  internal conversion in increasing  $\Delta E$  from 4200 to 6300  $\text{cm}^{-1}$ . This explanation is consistent with the different emission characteristics of dodecahexaene and tetradecaheptaene and fits within the  $1^1B_u^+ > 2^1A_g^-$  picture of polyene excited states.

The results presented in this paper allow us to consider the photophysical characteristics of polyenes longer than tetradecaheptaene. Extending the conjugation to  $n > 5$  should lead to the following: (1) a larger  $S_2-S_1$  ( $1^1B_u^+-2^1A_g^-$ ) energy gap—Figure 4 indicates  $\Delta E > 6300 \text{ cm}^{-1}$  in nonpolar solvents with a 600–700  $\text{cm}^{-1}$  increase in  $\Delta E$  for each additional double bond; (2) a smaller rate of  $S_2 \xrightarrow{\text{w}} S_1$  internal conversion—this rate should show an approximately exponential dependence on  $\Delta E$  ("weak coupling" limit of Englman and Jortner);<sup>35</sup> and (3) the relative dominance of  $S_2 \rightarrow S_0$  fluorescence—both  $S_2 \rightarrow S_0$  and  $S_1 \rightarrow S_0$  emission yields decrease with increasing  $n$ ; for very long polyenes  $S_2 \xrightarrow{\text{w}} S_0$  and  $S_1 \xrightarrow{\text{w}} S_0$  should be the primary routes for excited-state relaxation (Englman and Jortner).<sup>35</sup>

These trends suggest that for polyenes with  $n > 5$  (e.g.,  $\beta$ -carotene,  $n = 9$ ),  $S_2$  ( $1^1B_u^+$ ) and  $S_1$  ( $2^1A_g^-$ ) will be essentially "noncommunicating". For these molecules, population of  $S_1$  will only occur via direct excitation ( $1^1A_g^- \rightarrow 2^1A_g^-$ ) or by intermolecular energy transfer which avoids  $S_2$ . This opens up some interesting possibilities for long polyene photochemistries. For example, the light harvesting role of carotenoids in photosynthetic systems<sup>6</sup> would not require  $S_1(\text{carotene}) > S_1(\text{chlorophyll})$  but could be carried out by direct energy transfer from  $S_2(\text{carotene})$  to  $S_1(\text{chlorophyll})$ . A previous investigation<sup>7</sup> of the Raman excitation profile of  $\beta$ -carotene had led to the identification of some weak spectral features at  $\sim 18000 \text{ cm}^{-1}$  as vibronic bands of  $2^1A_g^-$ . This assignment places  $2^1A_g^-$  well above the  $\sim 15000\text{-cm}^{-1}$  origin of the lowest energy absorption in chlorophyll.<sup>38</sup> It also results in a  $S_2-S_1$  ( $1^1B_u^+-2^1A_g^-$ ) energy gap of  $\sim 3500 \text{ cm}^{-1}$  and thus cannot be reconciled with the energy differences given in Figures 4 and 5. If  $\Delta E$  for  $\beta$ -carotene is at least as large as the  $6300\text{-cm}^{-1}$  gap observed for tetradecaheptaene, then the assignment of  $\beta$ -carotene's Raman excitation profile is incorrect. This results in a revised energy scheme:  $S_2(\text{carotene}) > S_1(\text{chlorophyll}) > S_1(\text{carotene})$ . The relatively slow rate of  $S_2(\text{carotene}) \xrightarrow{\text{w}} S_1(\text{carotene})$  internal conversion would allow carotenoids to collect and transfer energy to photosynthetic reaction centers via  $S_2$ . This would have some advantages in that  $S_2$  is efficiently populated ( $S_0 \rightarrow S_2$  is an allowed transition) and can transfer its energy over large distances by Coulombic interactions.<sup>39</sup>

The revised energy scheme also furnishes a simple explanation of  $\beta$ -carotene's ability to quench chlorophyll fluorescence.<sup>40</sup>

Previous explanations start with the assumption that  $S_1(\text{chlorophyll}) < S_1(\beta\text{-carotene})$ . This precludes energy transfer and leads to a mechanism in which quenching occurs via electron transfer from carotene to chlorophyll. The revised energy scheme favors energy transfer over electron exchange and accounts for  $\beta$ -carotene's unique (and seemingly contradictory) ability to both sensitize and quench chlorophyll fluorescence. More work is needed to firmly establish the location of  $2^1A_g^-$  in  $\beta$ -carotene and other long polyenes, but the large  $S_2-S_1$  energy differences and the small  $S_2 \xrightarrow{\text{w}} S_1$  internal conversion rates both must be considered in modeling the photochemistries of these systems.

## V. Summary and Conclusions

*all-trans*-Tetradecaheptaene does not exhibit the large Stokes shift between absorption ( $1^1A_g^- \rightarrow 1^1B_u^+$ ) and fluorescence which is the hallmark of shorter polyene hydrocarbons. Solvent shift studies and fluorescence excitation spectra lead to the identification of two distinct fluorescences,  $S_2 \rightarrow S_0$  ( $1^1B_u^+ \rightarrow 1^1A_g^-$ ) and  $S_1 \rightarrow S_0$  ( $2^1A_g^- \rightarrow 1^1A_g^-$ ), and establish tetradecaheptaene as the first linearly conjugated molecule to violate Kasha's rule.

Tetradecaheptaene's dual emissions, like the anomalous fluorescences from azulene and other polyarenes, can be explained by the relative large energy difference between  $S_1$  and  $S_2$  ( $\sim 6300 \text{ cm}^{-1}$  in nonpolar solvents). This apparently slows  $S_2 \xrightarrow{\text{w}} S_1$  internal conversion relative to the rate of fluorescent decay from  $S_2$  ( $10^{11}\text{--}10^{12} \text{ s}^{-1}$ ). The relative emission yields from  $S_1$  and  $S_2$  are sensitive to solvent polarizability and confirm the increase in  $S_2$  fluorescence with increasing  $\Delta E$ . A more quantitative investigation of these effects would be useful in evaluating whether the theoretical treatments of radiationless transitions in cyclic aromatic hydrocarbons also apply to the linear polyenes.

The location of  $1^1B_u^+$  and  $2^1A_g^-$  in tetradecaheptaene extends our previous study of shorter polyenes and indicates the approximately linear divergence of these states with increasing conjugation. This behavior is not accounted for by current theoretical descriptions of polyene excited states. Further work will be needed to better establish  $2^1A_g^-$ 's long polyene energy limit. Nevertheless, the apparent disconnection between  $S_1$  and  $S_2$  for polyenes with  $\Delta E > 6000 \text{ cm}^{-1}$  points to some interesting spectroscopic and photochemical possibilities. For example, gas-phase octatetraene ( $\Delta E = 6400 \text{ cm}^{-1}$ ) exhibits resonance fluorescence ( $1^1B_u^+ \rightarrow 1^1A_g^-$ ) upon excitation of  $1^1B_u^+$ . This has led to the proposal that the low-lying  $2^1A_g^-$  state (only observed in solutions and low-temperature mixed crystals) may be an artifact of condensed-phase measurements. Our results indicate a greatly diminished rate of  $S_2 \xrightarrow{\text{w}} S_1$  internal conversion and imply that detection of  $2^1A_g^-$  in gaseous octatetraene may require direct excitation or intermolecular energy transfer which avoids  $S_2$ . The spectroscopic and kinetic energy trends discussed here also account for the ability of carotenoids to act both as donors and acceptors in energy-transfer processes involving chlorophyll. The light harvesting role of carotenoids in photosynthesis may be explained by  $S_2(\text{carotene}) > S_1(\text{chlorophyll}) > S_1(\text{carotene})$ . The extrapolation of our data on shorter polyenes to this energy scheme, however, clearly requires further experimental and theoretical attention.

**Acknowledgment.** This research was supported by a Penta Corporation Grant of Research Corporation, the donors of the Petroleum Research Fund, administered by the American Chemical Society, and a DuPont Fund Grant to Bowdoin College.

**Registry No.** *all-trans*-1,3,5,7,9,11,13-Tetradecaheptaene, 13020-66-1; *all-trans*-1,3,5,7,9,11-dodecahexaene, 13020-64-9.

(38) Thrash, R.; Fang, H.; Leroi, G. *Photochem. Photobiol.* **1979**, *29*, 1049.

(39) Turro, N. "Modern Molecular Photochemistry"; Benjamin/Cummings: Menlo Park, 1978; pp 296–361.

(40) Beddard, G.; Davidson, R.; Trethewey, K. *Nature (London)* **1977**, *267*, 373.